

# Dislocation mediated melting near isostructural critical points

T. Chou and David R. Nelson

*Department of Physics, Harvard University, Cambridge, MA 02138*

(February 6, 2018)

We study the interplay between an isostructural critical point and dislocation mediated two-dimensional melting, using a combination of Landau and continuum elasticity theory. If dislocations are excluded, coupling to the elastic degrees of freedom leads to mean field critical exponents. When dislocations are allowed, modified elastic constants lead to a new phase buried in the solid state near the critical point. Consistent with a proposal of Bladon and Frenkel, we find an intervening hexatic phase near the critical point of the first-order isostructural transition line. Very close to the critical point, a transition from the hexatic phase to a modulated bond angle state is possible. Ising transitions in symmetrically confined two dimensional colloidal crystals with attractive wall potentials require a different model free energy, which we also discuss.

## I. INTRODUCTION

First order phase transitions preserving symmetry and possessing a critical point have been well understood for many years, the most common example being the discontinuous liquid-vapor phase transition. Such systems can be brought continuously from one phase to another by taking a thermodynamic path which passes around the critical point along the equation of state surface without sudden changes in density. Near the critical point, liquid-vapor systems show critical opalescence among other properties peculiar to second order phase transitions.

Recently, attention has been focussed on *solid-solid* phase transitions [1–3]. Especially interesting are isostructural transitions in which the lattice spacing jumps discontinuously, but the symmetry of the lattice remains unchanged. A schematic phase diagram as a function of temperature,  $T$ , and particle density,  $\rho$ , is shown in Figure 1. As in the liquid-vapor transition, isostructural transitions can have a critical point above which the distinction between the isostructural phases  $S_1$  and  $S_2$  vanishes. Because the solid-solid coexistence region is on the higher density (solid) side of the fluid-solid coexistence region, a fluid-solid-solid triple point becomes possible.

Experimentally, bulk isostructural transitions have been observed in high pressure studies of Zr. Above the  $\text{fcc} \rightarrow \omega$  (at 6.7 GPa) and  $\omega \rightarrow \text{bcc}$  (at 33GPa) transitions, a lattice symmetry preserving transition between two bcc phases occurs at 53GPa [4]. Another experimentally convenient system with which to study solid-solid transitions is colloidal particles. Colloids are often observed to be in an ordered fcc or bcc lattice, useful for example, in colloidal array filters [5]. The interaction potential between colloid particles can be chemically tailored to control the range of interactions. For example, one can vary the length of grafted polymers, or change solvent properties [6]. Single layers of colloids can be confined to study the transitions of 2D solids. This has been achieved by squeezing colloidal particles between two flat plates [8] or floating them at an air-water interface [9].

The theoretical study of the statistical mechanics of colloidal particles has utilized various analytical [3,10–12] and numerical [13,14] methods. It is well established that hard spheres, with or without a superimposed attractive potential, can undergo a solid-fluid phase transition. When the attractive potentials are short-ranged enough, experiments and theory demonstrate that the liquid-gas coexistence vanishes [14,15]. The short-ranged attractive potentials required can be achieved with colloidal particles or in computer simulations. A recent numerical study [2] using particles with very short-ranged attractive potentials (attractive region  $< 7\%$  of the hard core diameter), and at high densities, show solid-solid phase coexistence. This behavior is consistent with the variational treatment of Tejero *et. al.* [3]

In this paper, we explore how ideas of defect mediated melting [16] may be incorporated into the schematic phase diagram of particles with short-ranged attractions. There is some evidence for a two-stage dislocation mediated melting process in liquid crystals [17], colloidal dispersions [8], and magnetic bubble domains [18], however, a first order transition from solid to liquid (for example by generation of grain boundaries) is also possible [19]. The study of defects away from an inherent solid-fluid transition, deep in the solid phase, near a solid-solid critical point, is a new opportunity to test predictions of dislocation melting theory [16].

As pointed out by Bladon and Frenkel [2], an intervening hexatic phase (the product of the first stage in the two-stage melting scenario) is likely near a two-dimensional isostructural critical point. Chen *et. al.*, studying an isothermal, isobaric Lennard-Jones system, point out the large system sizes required in searching for a metastable hexatic phase [20]. Nevertheless, simulation measurements of elastic constants by Bladon and Frenkel [2] show that a dislocation instability (presumably leading to a hexatic phase) *must* develop in the vicinity of a solid-solid critical point. Since the compressibility diverges near the critical point in Figure 1, the effective bulk modulus must soften [2]. This softening of the bulk modulus promotes dislocation unbinding which signals the solid-hexatic transition. In this

paper, we explore these ideas using a simple physical model and determine how the existence of a solid-solid critical point may induce a nearby hexatic phase. The effects of elastic degrees of freedom on the Ising critical properties in the *absence* of dislocations are also considered.

Finally, even though most simulations exhibiting a solid-solid phase transition rely on a very short-ranged attractive potential, longer-ranged, soft potentials may also show similar behavior. For example, the three-dimensional solid-solid transition in dense Cs and Ce [21] may be pressure induced [1,22]. Two-dimensional realizations such as confined colloids [8] and colloids [9] or  $C_{60}$  particles [23] at air-liquid interfaces also possess complicated short and long-ranged interactions. However, the *two-dimensional* melting outlined relies only on a solid-solid critical point and is not sensitive to the microscopic mechanism of particle interactions.

In the next section, we introduce two free energy functionals including both elastic degrees of freedom and the Ising-like order parameter describing the isostructural solid-solid phase transition. Elastic deformations and the Ising order parameter are coupled via an interaction energy. We also briefly discuss symmetrically confined colloidal crystals in 2D with attractive wall potentials. If the wall potential leads to an Ising-like symmetry-breaking, such that the crystal prefers to be near one wall or the other, a new type of isostructural critical point becomes possible.

Section III discusses the simplest model in the absence of defects. Above the critical point, the Ising degrees of freedom renormalize the elastic coefficients yielding an effective bulk modulus. Thermal fluctuations in the (single-valued) strains renormalize the critical temperature of the Ising degrees of freedom. We show that the critical temperature renormalization is different for the uniform and finite wavevector modes in a manner such that the Ising critical point acquires *mean-field* behavior. The uniform, zero wavevector strains induce an infinite-ranged interaction that insures *classical* critical exponents in this two-dimensional system.

In Section IV, the strains and Ising order parameter in the presence of a single dislocation are studied by solving the extremal (Euler) equations. The strain field configurations are asymptotically identical to those of an uncoupled model except they are functions of effective elastic coefficients. The related Ising order parameter near the dislocation is also determined. An energy-entropy argument for an isolated dislocation leads to the melting criterion simulated by Bladon and Frenkel [2]. Qualitative phase diagrams containing solid and hexatic phases are derived based on this criterion.

The free energy of the full interacting model is expressed in terms of a collection of *many* dislocations in Section V. Renormalization group flows for the the parameters in the presence of a few dislocations are also derived. Dislocation-renormalized elastic moduli yield a melting criterion agreeing with simple energy-entropy considerations. The critical exponents of the crystal-hexatic transition are the same as for conventional dislocation-mediated melting. [28,29]

Section VI explores transitions of the *hexatic* phase induced by the critical point. A modulated hexatic phase is possible very near the critical point. If there are no modulated hexatic instabilities, the coupling of the Ising order parameter to the hexatic bond angle field leaves the nontrivial Onsager-like critical behavior of the 2D critical point intact.

## II. FREE ENERGY MODELS

In this section we describe the free energy functional for the physics near an isostructural critical point in terms of the elastic strain fields, an Ising-like structural order parameter, and an interaction between these degrees of freedom. Dislocations, leading to multiple-valued displacement fields will only be considered in detail in later sections. Symmetries dictate the form of possible coupling terms.

A first order transition in a scalar quantity such as density near a critical point can be described by an Ising model. In the continuum representation, the “Landau-Ginzburg-Wilson” expression for the free energy takes the form [25]

$$\mathcal{H}_I \equiv \frac{F_I}{k_B T} = \int d^2x \left( \frac{1}{2} |\nabla\varphi|^2 + \frac{r}{2} \varphi^2 + \frac{u}{4!} \varphi^4 - h\varphi + \dots \right), \quad (2.1)$$

where for a first order liquid-gas transition or isostructural solid-solid transition,  $\varphi$  is defined as the density deviation from the critical density;  $\varphi = \rho - \rho_c$ . Near criticality,  $u$  is approximately independent of  $T$  and  $r \simeq a_2(T - T_c)/T_c$ . The linear term proportional to  $h$  represents a chemical potential and allows us to study the transitions at densities away from the critical isochore. Positive  $h$  favors  $\varphi > 0$  (*i.e.* the dense phase  $S_2$  in Fig. 1) while  $h < 0$  favors  $\varphi < 0$  (the dilute solid phase  $S_1$  in Fig. 1). A potential third order coupling, ( $w\varphi^3$ , say) in Equation (2.1) can be eliminated by a shift in  $\varphi$ .

In addition to an Ising order parameter describing the phase separation, a key feature of the solid phases is their resistance to deformations. The elastic deformation energy is [26],

$$\mathcal{H}_{el} \equiv \frac{F_{el}}{k_B T} = \frac{1}{2} \int d^2x (2\mu e_{ij}^2 + \lambda e_{ii}^2) \quad (2.2)$$

where  $e_{ij} = \frac{1}{2}(\partial_i u_j + \partial_j u_i)$  is the symmetric strain tensor and  $\mu$  and  $\lambda$  are the Lamé coefficients defined as the microscopic Lamé coefficients divided by  $k_B T$ . Equation (2.2) is valid for two-dimensional triangular crystals undergoing small strains.

The free energy (2.2) in general contains both smoothly varying single-valued strains as well as singular contributions from point-like defects such as dislocations. When a solid is thermally excited, defect complexions must be explicitly included in the statistical weight  $e^{-\mathcal{H}_{el}}$ , as well as in a coupling term, such as Eq. (2.3) below. As discussed in Sections IV and V, dislocations can be incorporated by considering the strains as comprised of a smooth “phonon” component,  $u_{ij}$ , and a singular part,  $w_{ij}$ , due to the presence of defects, so that  $e_{ij} = u_{ij} + w_{ij}$ .

We now consider the coupling between the order parameter  $\varphi$  and the strain. Since the model is isotropic, symmetry requires that to leading order, only the dilatation,  $e_{\ell\ell}$ , couples to the phase variable. The lowest order interaction term for a phase separating system is

$$\mathcal{H}_{int} = g \int d^2x \varphi e_{\ell\ell}. \quad (2.3)$$

We assume  $g > 0$  so that a lattice compression ( $e_{\ell\ell} < 0$ ) will bias the system toward  $\varphi > 0$ , *i.e.* toward the denser isostructural solid  $S_2$  in Figure 1. Related couplings between an elastic strain field and an auxiliary field have been studied in the context of compressible statistical spin models [30,31], quenched random impurities [32], and vacancy/interstitial defects in crystals.

For compressible magnets with an Ising-like order parameter, the relevant interaction energy is [30,31]

$$\mathcal{H}_{int} = g' \int d^2x \varphi^2 e_{\ell\ell}. \quad (2.4)$$

A model of this kind would be appropriate for colloidal crystals symmetrically confined between glass plates with attractive wall potentials of the kind shown in Figure 2. Such a double wall potential can induce (for the appropriate pair potentials between the colloidal particles) an Ising-like isostructural critical point inside the two-dimensional crystalline phase. Below the Ising phase transition, the crystal prefers to sit closer to one wall or the other. If  $\varphi(\vec{x})$  represents the deviation of the local particle position from the mid-plane, we can use Eq. (2.1) (with  $h = 0$ ) to represent the Ising degrees of freedom and Eq. (2.2) to model the elastic ones. The symmetrical confinement (we neglect gravity) insures that a coupling of the form (2.3) is impossible, so we are left with (2.4).

As discussed, for example, by Bergman and Halperin [30], this coupling changes the critical exponents of the Ising-like transition in the *absence* of dislocations provided the specific heat exponent  $\alpha$  of the pure Ising system is positive. Because  $\alpha = 0$  for the 2D Ising model, there is at most a very slow marginal crossover away from pure Ising-like behavior for these symmetrically confined crystals. The coupling  $g'$  induces a specific heat-like singularity in the inverse elastic bulk modulus  $\bar{B}^{-1}$  near the transition. The renormalized inverse bulk modulus can be defined as

$$\begin{aligned} \frac{1}{\bar{B}} &= \frac{1}{A} \langle U_{ii} U_{jj} \rangle \\ &= \frac{1}{B} + \frac{g'^2}{B^2} \frac{1}{A} \int d^2x d^2x' \langle \varphi^2(\vec{x}) \varphi^2(\vec{x}') \rangle \simeq \frac{1}{B} + a_2 \frac{g'^2}{B^2} \left( \frac{T - T_c}{T_c} \right)^{-\alpha}, \end{aligned} \quad (2.5)$$

where  $U_{ii} = \int d^2x u_{ii}(\vec{x})$ ,  $A$  is the system area, and  $B \equiv \mu + \lambda$ . If the specific heat diverges,  $\bar{B} = 0$ , the energy of one isolated dislocation will become small, and we again expect dislocation mediated melting close to the critical point, similar to the argument in Ref. [2]. However, this specific heat singularity is much weaker than the singularity which induces melting for an asymmetrical model, so a hexatic phase may be difficult to observe experimentally.

In the remainder of this paper, we consider only the linear coupling, (2.3) where the effects are expected to be more dramatic. The total free energy is thus,

$$\mathcal{H} = \int d^2x \left[ \mu e_{ij}^2 + \frac{\lambda}{2} e_{ii}^2 \right] + g \int d^2x e_{\ell\ell} \varphi + \int d^2x \left[ \frac{1}{2} |\nabla \varphi|^2 + \frac{r}{2} \varphi^2 + \frac{u}{4!} \varphi^4 - h \varphi + \dots \right]. \quad (2.6)$$

Figure 3 shows schematically the coexistence of two different density phases of lattice constant  $a_+$  and  $a_-$ . Under a uniform area change, the system responds by undergoing both pure dilatational elastic deformations in each of the phases as well as interconversion between local regions of phase,  $S_1$  or  $S_2$ . The relative partition between these two responses is governed by  $g$ . In Appendix A, we discuss the stability constraints on the coupling constants determined from Eq. (2.6) expanded to quadratic order.

### III. DEFECT-FREE LIMIT

In this section, we study the interplay between the strain and Ising fields in the absence of defects. The strain fields  $u_{ij}$  are single-valued and can be thermally averaged out in the quadratic theory. We assume free boundary conditions in the  $(x_1, x_2)$  - plane and write the Fourier transformed strain in terms of uniform bulk distortions and finite wavevector modes [34]

$$u_{ij}(\vec{x}) = u_{ij}^{(0)} + \frac{1}{2A} \sum_{\vec{q} \neq 0} i(q_i u_j(\vec{q}) + q_j u_i(\vec{q})) e^{i\vec{q} \cdot \vec{x}}. \quad (3.1)$$

In the decomposition (3.1), the uniform symmetric strains  $u_{ij}^{(0)}$  must be treated separately because these require *three* degrees of freedom, in contrast to the two independent phonon modes which arise when  $\vec{q} \neq 0$ . A similar treatment is required in the study of the zero-wavevector excitation in Bose-Einstein condensation.

Similar to (3.1), we decompose  $\varphi(\vec{x})$  as

$$\begin{aligned} \varphi(\vec{x}) &= \varphi_0 + \sum_{\vec{q} \neq 0} \tilde{\varphi}(\vec{q}) e^{i\vec{q} \cdot \vec{x}} \\ &= \varphi_0 + \delta\varphi(\vec{x}). \end{aligned} \quad (3.2)$$

For the linear coupling model (2.3) considered here, the zero wavevector strain modes couple only to the zero wavevector Ising field  $\varphi_0$ . After integrating out these uniform bulk strains, we find an effective energy for  $\varphi_0$ . Averaging over the fluctuating crystal displacements,  $(\vec{u}(\vec{q}), \vec{q} \neq 0)$ , however, gives a different effective energy for the nonzero wavevector Ising fields  $\delta\varphi(\vec{x})$ . The final result including the quartic coupling is

$$\begin{aligned} \mathcal{H}_{eff}[\varphi] &= A \left[ \left( \frac{r}{2} - \frac{g^2}{2B} \right) \varphi_0^2 + \frac{u}{4!} \varphi_0^4 - h\varphi_0 \right] + \frac{1}{2} \int d^2x \left[ |\vec{\nabla}\varphi|^2 + \left( r - \frac{g^2}{(\mu+B)} + \frac{u}{2} \varphi_0^2 \right) \delta\varphi^2(\vec{x}) \right] \\ &\quad + \frac{u}{6A^3} \varphi_0 \sum_{\vec{q}_1 \neq 0} \sum_{\vec{q}_2 \neq -0, \vec{q}_1} \varphi(\vec{q}_1) \varphi(\vec{q}_2) \varphi(-\vec{q}_1 - \vec{q}_2) + \frac{u}{4!} \int d^2x \delta\varphi^4(\vec{x}) + \dots \end{aligned} \quad (3.3)$$

where  $\delta\varphi(\vec{x})$  contains only finite wavevector perturbations of the Ising order parameter about its uniform value  $\varphi_0$ .

The  $\vec{q} = 0$  strains ( $u_{ij}^{(0)}$ ) renormalize the  $\varphi_0$  modes differently than the finite wavevector phonons ( $\vec{u}(\vec{q})$ ), renormalize the  $\varphi(\vec{q} \neq 0)$  modes. The critical temperature of  $\varphi_0$  is shifted according to  $T^* \approx T_c(1 + g^2/a_2B)$ . The mass or quadratic coefficient of the  $\varphi_0$  field (denoted  $\bar{r}_0$ ), will, upon decreasing temperature, always vanish before the quadratic coupling of the finite wavevector modes, (denoted  $\bar{r}$ ). Thus,  $\bar{r}_0 < \bar{r}$ , where

$$\bar{r}_0 \equiv r - \frac{g^2}{B} \quad (3.4)$$

and,

$$\bar{r} \equiv r - \frac{g^2}{(\mu+B)} + \frac{u}{2} \varphi_0^2. \quad (3.5)$$

Since the  $\delta\varphi(\vec{x})$  modes remain massive near  $\bar{r}_0 \approx 0$ , they can be integrated out in perturbation theory to give a renormalized effective potential (with no gradient term) for the remaining  $\varphi_0$  degree of freedom. It is easily checked that the ordering of  $\varphi_0$  prevents the subsequent ordering of the  $\delta\varphi(\vec{x})$  modes at a lower temperature within our model. We conclude that the critical behavior of a 2D Ising model interacting with strain fields according to Eq. (2.3) is described by *mean-field* exponents.

The physical reason for mean-field critical behavior is that the uniform strains induce an infinite-ranged interaction between the zero wavevector Ising degrees of freedom. To see this, note that the quadratic contributions to Eq. (3.3) may be combined to give

$$\mathcal{H}_{eff}^{(2)} = \frac{1}{2} \int d^2x \left[ |\nabla\varphi(\vec{x})|^2 + \left( r - \frac{g^2}{\mu+B} \right) \varphi^2(\vec{x}) \right] - \frac{\mu g^2}{A(\mu+B)B} \int d^2x \int d^2x' \varphi(\vec{x}) \varphi(\vec{x}'). \quad (3.6)$$

The first term is the usual continuum representation of a short-ranged interaction, but the second has infinite range, induced by the strain coupling.

It is also instructive to consider elastic constants as renormalized by fluctuations of the Ising variable. It is easy to show that integrating over the slowly varying  $\varphi$  degrees of freedom leads to an effective Lamé coefficient

$$\bar{\lambda} = \lambda - g^2/r', \quad (3.7)$$

where

$$r' = r + \frac{u}{2}\varphi_0^2. \quad (3.8)$$

Consider the behavior of the effective elastic constant  $\bar{\lambda}$  near the (mean field) critical temperature  $T^*$  discussed above. Recall that  $\bar{r}_0(T^*) = 0$ , and let us assume for simplicity that  $h = 0$  and  $T \leq T^*$ . Since  $r' = r$  in this case, we have  $r'(T^*) = r(T^*) = g^2/B = g^2/(\mu + \lambda)$ . It follows that

$$\bar{\lambda}(T^*) = -\mu \quad (3.9)$$

so that the effective bulk modulus

$$\bar{B}(T) = \mu + \bar{\lambda} \quad (3.10)$$

vanishes as  $T \rightarrow T^*$ . This vanishing of the effective bulk modulus is expected quite generally, since  $\bar{B}$  is related to the Ising fluctuations in our model by an equation similar to (2.5), namely,

$$\begin{aligned} \frac{1}{\bar{B}} &= \frac{1}{A} \langle U_{ii} U_{jj} \rangle \\ &= \frac{1}{B} + \frac{g^2}{B^2} \frac{1}{A} \int d^2x \int d^2x' \langle \varphi(\vec{x}) \varphi(\vec{x}') \rangle. \end{aligned} \quad (3.11)$$

The strongly divergent mean field Ising fluctuations,  $\frac{1}{A} \int d^2x \int d^2x' \langle \varphi(\vec{x}) \varphi(\vec{x}') \rangle \sim (T - T^*)^{-1}$ , insure that  $\bar{B}$  vanishes. The reduction in  $\lambda$  implied by (3.7) corresponds to a lattice softening, suggesting that dislocations can more easily form.

Linear stability analysis of the defect-free model is given in Appendix A. The conditions of stability are different for zero wavevector and finite wave vector instabilities consistent with the renormalized “masses” for  $\vec{q} = 0$  and  $\vec{q} \neq 0$  fluctuations,  $\bar{r}_0$  and  $\bar{r}$ , respectively.

#### IV. ISOLATED DISLOCATION

In this Section, we determine the behavior of  $\varphi$  and the strains with a single dislocation at the origin. We also calculate the free energy of this dislocation and apply an energy-entropy balance to predict when dislocations are favored. The dislocation contribution to the field configurations is found by solving the extremal equations developed below.

We first write the total strain as

$$e_{ij} = u_{ij}^{(0)} + w_{ij} \quad (4.1)$$

where  $u_{ij}^{(0)}$  is the  $\vec{q} = 0$  part and  $w_{ij}$  are the singular strains due to the dislocation. After minimizing with respect to  $u_{ij}^{(0)}$  and expanding  $\varphi(\vec{x})$  about a uniform value  $\varphi_0 + \delta\varphi(\vec{x})$ , we find that the effective free energy becomes (to quadratic order in  $\delta\varphi$ )

$$\mathcal{H}_{\text{eff}}[\varphi, w_{ij}] = A \left[ \frac{\bar{r}_0}{2} \varphi_0^2 + \frac{u}{4!} \varphi_0^4 - h \varphi_0 \right] + \int d^2x \left[ \mu w_{ij}^2 + \frac{\lambda}{2} w_{ii}^2 + g \delta\varphi w_{ii} + \frac{1}{2} |\nabla \delta\varphi|^2 + \frac{r'}{2} \delta\varphi^2 + O(\delta\varphi^3) \right], \quad (4.2)$$

where  $\bar{r}_0$  is given by Eq. (3.4) and  $r'$  is given by Eq. (3.8). Near a dislocation  $\varphi$  distorts from  $\varphi_0$ . We will assume that  $\varphi(\vec{x} \rightarrow \infty) \rightarrow \varphi_0$ , where  $\varphi_0$  is one of possibly two uniform minima. This *ansatz* is appropriate in the presence of a single dislocation, since domain walls connecting regions with  $\varphi = \varphi_0$  and  $\varphi = -\varphi_0$  would cost an additional gradient energy scaling as the system size.

After minimizing (4.2) with respect to  $\varphi_0$ ,  $\delta\varphi(\vec{x})$ , and  $\vec{u}$ , the displacement caused by the dislocation, we obtain

$$\bar{r}_0 \varphi_0 + \frac{u}{6} \varphi_0^3 - h + \frac{u}{2} \varphi_0 \int d^2x \delta\varphi^2(\vec{x}) = 0, \quad (4.3)$$

$$-\nabla^2\delta\varphi + r'\delta\varphi + gw_{ii} + O(\delta\varphi^2) = 0, \quad (4.4)$$

and,

$$\mu\nabla^2\vec{u} + (\mu + \lambda)\vec{\nabla}(\vec{\nabla} \cdot \vec{u}) + g\vec{\nabla}\delta\varphi = -\mu\hat{z} \times \vec{b}\delta(\vec{x}), \quad (4.5)$$

where  $\vec{u}$  in the last equation is understood to be the lattice displacement due to the dislocation,  $w_{ij} = \frac{1}{2}(\partial_i u_j + \partial_j u_i)$ . These strains which satisfy the extremal equations guarantee vanishing of cross terms between  $u_{ij}$  and  $w_{ij}$  in (4.2). We the treatment in Ref. [26] and write the displacement vector as  $\vec{u} = \vec{u}_0 + \vec{u}'$ , where  $\vec{u}_0$  assumes the Burger's vector when integrated around a dislocation, *i.e.*,  $\nabla^2\vec{u}_0 = -\hat{z} \times \vec{b}\delta(\vec{x})$ . Note also that  $\nabla \cdot \vec{u}_0 = 0$ . By taking the divergence of (4.5) and substituting in the expression for  $(\vec{\nabla} \cdot \vec{u})$  from (4.4), we obtain a closed equation for  $\delta\varphi(\vec{x})$ ,

$$-\nabla^4\delta\varphi + \left(r' - \frac{g^2}{\mu + B}\right)\nabla^2\delta\varphi = \frac{2\mu g}{\mu + B}\nabla \cdot \hat{z} \times \vec{b}\delta(\vec{x}). \quad (4.6)$$

Note that we have retained the gradient contribution to the energy in Eq. (4.4). The value of  $\varphi_0$  must be determined self-consistently; however, for small  $\delta\varphi(\vec{x})$ , the correction to  $\bar{r}_0$  in (4.3) is small, and  $\varphi_0$  can be approximated by the solution to

$$\bar{r}_0\varphi_0 + \frac{u}{6}\varphi_0^3 - h \approx 0. \quad (4.7)$$

Having determined the boundary conditions for a single dislocation at the origin, we can solve for a small deviation of the Ising order parameter  $\delta\varphi(\vec{x})$ . With  $\vec{x} = \{x_1, x_2\}$ , and  $\vec{b} = b\hat{e}_1$ , where  $\hat{e}$  is a unit vector in the  $x_1$  direction,

$$\delta\varphi(\vec{x}) \simeq \frac{\mu gb}{\pi\kappa^2(\mu + B)} \frac{x_2}{|\vec{x}|^2} \left[1 - \sqrt{\frac{\pi}{2\kappa|\vec{x}|}} e^{-\kappa|\vec{x}|}\right]. \quad (4.8)$$

where

$$\begin{aligned} \kappa^2 &= \bar{r} \\ &= r' - \frac{g^2}{\mu + B}. \end{aligned} \quad (4.9)$$

A plot of  $\delta\varphi(\vec{x})$  is shown in Figure 4. The peaks and valleys ( $x_2 > 0$  and  $x_1 < 0$  respectively) correspond to a missing or extra row of particles. We also calculate the dilatation, Eq. (4.4);

$$\nabla \cdot \vec{u} = w_{ii} \simeq -\frac{\mu br'}{\pi\kappa^2(\mu + B)} \frac{x_2}{|\vec{x}|^2} \left[1 - O(|\vec{x}|^3 e^{-\kappa|\vec{x}|})\right] \quad (4.10)$$

which is asymptotically inversely proportional to  $\delta\varphi$ . The total displacements can be found from

$$\mu\nabla^2\vec{u}' = -(\mu + \lambda)\vec{\nabla}w_{ii} - g\vec{\nabla}\delta\varphi - 2\mu b\delta(\vec{x})\hat{e}_2. \quad (4.11)$$

We note that  $\partial w_{ii}/\partial x_2$  and  $\partial\delta\varphi/\partial x_2$  behave as  $\delta$ -functions at the origin, and find the total displacements around a dislocation,

$$\begin{aligned} u_1 &= \frac{b}{2\pi} \left[ \tan^{-1}\left(\frac{x_2}{x_1}\right) + \frac{Br' - g^2}{\kappa^2(\mu + B)} \frac{x_1 x_2}{|\vec{x}|^2} \right] + O(e^{-\kappa|\vec{x}|}) \\ u_2 &= -\frac{b}{2\pi} \left[ \frac{\mu r'}{\kappa^2(\mu + B)} \ell n|\vec{x}| + \frac{Br' - g^2}{\kappa^2(\mu + B)} \frac{x_1^2}{|\vec{x}|^2} \right] + O(e^{-\kappa|\vec{x}|}) \end{aligned} \quad (4.12)$$

These displacements are asymptotically identical to those of standard elasticity theory [26], except with  $\lambda$  replaced by  $\bar{\lambda}$ .

Evaluating (4.2) to quadratic order using asymptotic expressions for  $\vec{u}$  and  $\delta\varphi$  gives the total energy of a single dislocation of strength  $b$ :

$$\mathcal{H}_{eff} = \frac{\bar{K}b^2}{8\pi} \ell n\left(\frac{R}{a}\right) + c(a), \quad (4.13)$$

where  $R$  is the linear sample dimension and  $c(a)$  is function of the dislocation core size  $a$ . The most singular part of the energy (4.13) has the same form as the standard result except with effects of the coupling  $\mathcal{H}_{int}$  contained in an effective Young's modulus

$$\bar{K} = \frac{4\mu(\mu + \bar{\lambda})}{2\mu + \bar{\lambda}} \quad (4.14)$$

where the effective Lamé coefficient for a dislocation is given by

$$\bar{\lambda} = \lambda - \frac{g^2}{r'}, \quad (4.15)$$

consistent with Eq. (3.7). As discussed in Section III, this reduction of  $\lambda$  causes the effective bulk modulus  $\bar{B} = \mu + \bar{\lambda}$  to vanish near the isostructural critical point.

The total free energy of a dislocation,  $G_1$ , also includes entropy describing configurations associated with the  $(R/a)^2$  possible positions the dislocation can occupy. Hence,

$$G_1/k_B T = \mathcal{H}_{eff} - 2\ell n(R/a). \quad (4.16)$$

The temperature above which the entropy favors dislocation formation is given by  $G_1/k_B T \approx 0$ , or,

$$\bar{K} \approx 16\pi. \quad (4.17)$$

This criterion, modified from the Kosterlitz-Thouless criterion of the decoupled theory ( $4\mu B/(\mu + B) \approx 16\pi$ ) determines the phase diagram. The onset of dislocation melting occurs when  $K > \bar{K}$ , where

$$\begin{aligned} \bar{K} &= \frac{4\mu [Br' - g^2]}{(\mu + B)r' - g^2} \\ &= \frac{4\mu(\mu + \bar{\lambda})}{2\mu + \bar{\lambda}} = 16\pi. \end{aligned} \quad (4.18)$$

This condition is equivalent to the usual Kosterlitz-Thouless criterion, with the replacement  $B \rightarrow \bar{B} = B - g^2/r'$ . Because  $\bar{B}(T) \rightarrow 0$  as  $T \rightarrow T^*$ , melting is inevitable near the isostructural critical point. To obtain phase diagrams, we assume  $\mu$  and  $B$  to be slowly varying functions of the order parameter  $\varphi$ . If we further assume for simplicity that bare elastic constants (unrenormalized by either Ising order parameter fluctuations or dislocations) satisfy  $\mu(\rho_c) \approx \lambda(\rho_c)$ , the original dislocation mediated melting theory ( $g = 0$ ), predicts dislocation unbinding when  $\mu(\rho_c), \lambda(\rho_c) \approx 6\pi$ . However, in the modified Kosterlitz-Thouless criterion, (4.18), the effective parameters may be such that (4.18) is satisfied even when  $\mu, \lambda > 6\pi$ . In the  $(\bar{r}_0/u, \rho - \rho_c)$  plane, the boundary of a hexatic phase near the isostructural critical point as found from (4.18) is shown in Figure 1.

We use the solution of the cubic equation (4.7) in (4.18) to obtain a quantitative picture in the  $h - T$  plane. Phase boundaries for  $\mu = \lambda = 10\pi$  in the  $\bar{r}_0/u$  and  $h/u$  plane are plotted in Figure 6. More precise determination of the phase boundary would require a first principles calculation of the unrenormalized elastic moduli  $\mu$  and  $\lambda$ . This can be obtained for example by density functional theory [12] or primitive cell models [1]. Our simple model however, shows salient features of 2D melting induced by an isostructural critical point and agrees qualitatively with the simulated phase diagram of Bladon and Frenkel [2].

## V. EFFECTS OF MANY DISLOCATIONS

When many dislocations are present, the possibility of more complicated structures arises. In particular, dislocations may aggregate to form grain boundaries, or extended domains where  $\varphi$  may take on values different from  $\varphi_0$ , or for  $\bar{r}_0 < 0$ , both domains of  $+\varphi_0$  and  $-\varphi_0$  phases may coexist. We will assume these complex aggregates do not form. Here, we assume a dilute dislocation gas, and demonstrate that the renormalization group recursion relations for the effective parameters are unchanged from those of the uncoupled melting theory.

The stress tensor associated with  $\mathcal{H} \equiv \mathcal{H}_{el} + \mathcal{H}_I + \mathcal{H}_{int}$  is

$$\sigma_{ij} = (\mu + \lambda)e_{\ell\ell}\delta_{ij} + 2\mu(e_{ij} - \frac{1}{2}e_{\ell\ell}\delta_{ij}) + 2g\varphi\delta_{ij}, \quad (5.1)$$

which can be inverted to give

$$e_{ij} = \frac{1}{2\mu}\sigma_{ij} - \frac{\lambda}{4\mu(\mu + \lambda)}\sigma_{\ell\ell}\delta_{ij} - \frac{g}{\mu + \lambda}\varphi\delta_{ij}. \quad (5.2)$$

Functional minimization with respect to the phonon displacements yields a divergence-free stress,

$$\partial_i\sigma_{ij}^{(s)} = 0 \quad (5.3)$$

to which must be added single-valued fluctuating stresses  $\tilde{\sigma}_{ij}$ . Since (5.3) holds away from defects, the extremal stress can be expressed in terms of a double curl, [26]

$$\sigma_{ij}^{(s)} \equiv \epsilon_{im}\epsilon_{jn}\partial_m\partial_n\chi. \quad (5.4)$$

For the present problem, the stress tensor for a collection of dislocations at positions  $\{\vec{x}_\alpha\}$  with Burgers' vectors  $\{\vec{b}_\alpha\}$  and ‘‘Burger’s charge density’’  $\vec{b}(\vec{x}) = \sum_\alpha \vec{b}_\alpha\delta(\vec{x} - \vec{x}_\alpha)$  is given by

$$\begin{aligned} \sigma_{ij} &= \sigma_{ij}^{(s)} + \tilde{\sigma}_{ij} \\ &= -\frac{K_0}{4\pi}\epsilon_{im}\epsilon_{jn}\partial_m\partial_n \int d^2x' b_k(x')\epsilon_{kl}(x-x')_\ell \left[ \ln\frac{|\vec{x} - \vec{x}'|}{a} + C \right] \\ &\quad + \frac{gK_0}{\mu + \lambda}\epsilon_{im}\epsilon_{jn}\partial_m\partial_n \int d^2x' G(x-x')\nabla^2\varphi(x') + \tilde{\sigma}_{ij} \end{aligned} \quad (5.5)$$

where  $\nabla^4 G(\vec{x}) = \delta(\vec{x})$  and  $C$  is a constant of order unity. The functional form of the free energy  $\mathcal{H} = \frac{1}{2} \int d^2x \sigma_{ij} e_{ij} + \mathcal{H}_I$  becomes

$$\mathcal{H} = \mathcal{H}_I[\varphi] + \mathcal{H}_0[u_{ij}] + \mathcal{H}_{int}[\varphi, u_{ij}] + \mathcal{H}_D[\vec{b}] \mathcal{H}_{int}^{sing}[\varphi, \vec{b}] \quad (5.6)$$

where  $u_{ij}$  is the smoothly varying part of the strain and

$$\mathcal{H}_D = -\frac{K_0}{8\pi} \sum_{\alpha \neq \beta} \left[ \vec{b}(\vec{x}_\alpha) \cdot \vec{b}(\vec{x}_\beta) \ln\left(\frac{|\vec{x}_\alpha - \vec{x}_\beta|}{a}\right) - \frac{\vec{b}(\vec{x}_\alpha) \cdot (\vec{x}_\alpha - \vec{x}_\beta) \vec{b}(\vec{x}_\beta) \cdot (\vec{x}_\alpha - \vec{x}_\beta)}{|\vec{x}_\alpha - \vec{x}_\beta|^2} \right] + \frac{E_c}{k_B T} \sum_\alpha |\vec{b}(\vec{x}_\alpha)|^2. \quad (5.7)$$

The dislocation contribution to the strain,  $w_{ii}$ , may be written in terms of Burgers’ vectors [27,28,32],

$$w_{ii}(\vec{x}) = -\frac{K_0}{4\pi(\mu + \lambda)} \sum_\alpha \frac{\hat{z} \cdot \vec{b}(\vec{x}_\alpha) \times (\vec{x} - \vec{x}_\alpha)}{|\vec{x} - \vec{x}_\alpha|^2}, \quad (5.8)$$

which leads to

$$\begin{aligned} \mathcal{H}_{int}^{sing}[\varphi, \vec{b}] &= g \int d^2x w_{ii} \varphi \\ &= \frac{gK_0}{4\pi(\mu + \lambda)} \sum_\alpha \int d^2x \varphi(\vec{x}) \frac{\hat{z} \cdot \vec{b}(\vec{x}_\alpha) \times (\vec{x} - \vec{x}_\alpha)}{|\vec{x} - \vec{x}_\alpha|^2}. \end{aligned} \quad (5.9)$$

If the fluctuations in  $\delta\varphi(\vec{x})$  are now averaged out, the effective model of interacting dislocations takes the form of  $\mathcal{H}_D$ , except with the replacement  $K_0 \rightarrow \bar{K}$ , with  $\bar{K}$  given by (4.18). Although we have omitted the details, these results follow from straightforward generalizations of (4.3), (4.4), and (4.5). For example, (4.5) is generalized as

$$\mu\nabla^2\vec{u} + (\mu + \lambda)\vec{\nabla}(\vec{\nabla} \cdot \vec{u}) + g\vec{\nabla}\varphi = \mu \sum_\alpha \hat{z} \times \vec{b}_\alpha\delta(\vec{x} - \vec{x}_\alpha). \quad (5.10)$$

The energy (5.6) can be analyzed by rescaling dislocation core sizes and distances in a way similar to that discussed in [29]. Although recursion relations for  $g$  and  $r$  as well as the elastic coefficients can be found this way, it is simpler to construct recursion relations in terms of the effective coupling  $\bar{K}$ . These recursion relations are [28,29]

$$\frac{dy(\ell)}{d\ell} = \left[ 2 - \frac{\bar{K}(\ell)}{8\pi} \right] y(\ell) + 2\pi y^2(\ell) e^{\bar{K}(\ell)/16\pi} I_0(\bar{K}(\ell)/8\pi) + O(y^3(\ell)) \quad (5.11)$$



$$\frac{d\bar{K}^{-1}(\ell)}{d\ell} = \frac{3\pi}{2}y^2(\ell)e^{\bar{K}(\ell)/8\pi} \left[ I_0(\bar{K}(\ell)/8\pi) - \frac{1}{2}I_1(\bar{K}(\ell)/8\pi) \right] + O(y^3(\ell)) \quad (5.12)$$

where  $\bar{K}(\ell)$  is defined by (4.18) and  $y(\ell)$  is the dislocation fugacity  $y \simeq e^{-E_c/k_B T}$ .  $\bar{K}(\ell)$  and  $y(\ell)$  are the usual scale-dependent renormalization group coupling constants. The  $O(y^2)$  term on the right-hand-side of (5.11) is found by considering three dislocation configurations [28]. Flows of the parameters, as one considers increasing length scales  $\ell$ , which have  $y \rightarrow 0$  indicate states with proliferated dislocations, or a hexatic phase. A melting criterion identical with the modified Kosterlitz-Thouless criterion, Equation (4.18), arises from analysis of (5.11). Moreover, we conclude that the critical properties of standard dislocation melting theory [28], such as an essential singularity in the specific heat, and a divergence of the translational correlation length of the form  $\xi_+(T) \sim \exp(\text{const.}/|T - T_m|^{0.36963})$ , are unchanged from the result of the usual dislocation-mediated theory.

## VI. HEXATIC MELTING AND DISCLINATION UNBINDING

In this Section, we examine the stability of the critical-point-induced hexatic phase. Within the hexatic phase, when many dislocations are unbound, the free energy is described by slow spatial variations in the bond angle field [27,28]. The lowest order symmetry allowed coupling between the bond angle  $\theta$  and Ising order parameter has the form  $v\nabla\theta \cdot \nabla\varphi$ , and the total free energy is

$$\mathcal{H}_{hex} = \frac{K_A}{2} \int d^2x |\nabla\theta|^2 + v \int d^2x \nabla\theta \cdot \nabla\varphi + \mathcal{H}_I[\varphi], \quad (6.1)$$

where  $K_A$  is the hexatic stiffness constant;  $K_A(T) \rightarrow \infty$  as the freezing transition is approached from the hexatic phase [28]. We now consider the behavior of the bond angle and density order parameter in the presence of disclinations. The hexatic phase predicted from the standard dislocation melting theory will melt into an isotropic fluid phase upon further increase in temperature. Proliferating disclinations cause this first order transition.

For our model, (6.1), we find that the interactions between disclinations and  $\varphi$  fields decouple. To see this, we first write the extremal equations derived from (6.1);

$$K_A \nabla^2 \theta + v \nabla^2 \varphi = 0 \quad (6.2)$$

$$-\nabla^2 \varphi + r\varphi + \frac{u}{6}\varphi^3 - h - v \nabla^2 \theta = 0. \quad (6.3)$$

Note that Eq. (6.2) allows us to define a conjugate bond angle field

$$\epsilon_{ij} \partial_j \tilde{\theta} \equiv \partial_i \theta + \frac{v}{K_A} \partial_i \varphi. \quad (6.4)$$

The density order parameter is assumed to be single-valued; however, the bond angle  $\theta$  obeys the noncommutivity relation implied by a set of disclinations located at positions  $\{\vec{x}_\alpha\}$ ,

$$\epsilon_{ij} \partial_i \partial_j \theta = m(\vec{x}) = \frac{\pi}{3} \sum_\alpha s_\alpha \delta(\vec{x} - \vec{x}_\alpha). \quad (6.5)$$

The strength of the  $\alpha^{th}$  singularity is measured by the charge  $s_\alpha = \pm 1$ . Thus, we find

$$\partial_i \theta(\vec{x}) = \epsilon_{ij} \int d^2x' m(\vec{x}') \partial_j G(\vec{x} - \vec{x}') - \frac{v}{K_A} \partial_i \varphi(\vec{x}) \quad (6.6)$$

Using Eq. (6.6), we find that the terms coupling the disclination positions to  $\varphi(\vec{x})$  vanish and

$$\begin{aligned} \mathcal{H}_V = & \frac{-\pi K_A}{36} \sum_{\vec{x} \neq \vec{x}'} s(\vec{x}) s(\vec{x}') \ell n \frac{|\vec{x} - \vec{x}'|}{a} + \frac{E_c}{k_B T} \sum_{\vec{x}} s^2(\vec{x}) + \frac{K_A}{2} \int d^2x |\nabla \tilde{\theta}|^2 \\ & + v \int d^2x \nabla \tilde{\theta} \cdot \nabla \varphi + \int d^2x \left[ \frac{1}{2} |\nabla \varphi|^2 + \frac{r}{2} \varphi^2 + \frac{u}{4!} \varphi^4 - h\varphi \right], \end{aligned} \quad (6.7)$$

where  $\tilde{\theta}$  represents the smoothly varying part of the bond angle field. In addition to a possible disclination unbinding transition, a finite wavevector instability may develop when higher order terms in  $\nabla\varphi$  are included in (6.7). If we expand (6.7) to quadratic order about the minimum of  $\varphi$  and average over the smooth density fluctuations, we find

$$\begin{aligned} \mathcal{H}_V = & \frac{-\pi K_A}{36} \sum_{\vec{x} \neq \vec{x}'} s(\vec{x})s(\vec{x}') \ell n \frac{|\vec{x} - \vec{x}'|}{a} + \frac{E_c}{k_B T} \sum_{\vec{x}} s^2(\vec{x}) + \frac{K_A}{2} \int d^2x |\nabla\tilde{\theta}|^2 \\ & + \frac{\bar{K}_B}{2} \int d^2x |\nabla^2\tilde{\theta}|^2 + \frac{K_C}{2} \int d^2x |\nabla\nabla^2\tilde{\theta}|^2 \end{aligned} \quad (6.8)$$

where we have added higher order terms  $\frac{1}{2}K_B|\nabla^2\tilde{\theta}|^2$  and  $\frac{1}{2}K_C|\nabla\nabla^2\tilde{\theta}|^2$  to Eq. (6.7), and defined

$$\bar{K}_B \equiv K_B - \frac{v^2}{r + \frac{u}{2}\varphi_0^2}. \quad (6.9)$$

Either expression, (6.7) or (6.8), shows that the interaction energy in (6.1) decouples from the disclination configurations and only modifies the effective stiffness of the  $\varphi$  or  $\theta_0$  fields.

Note from Eq. (6.9) that  $\bar{K}_B$  becomes negative near the isostructural critical point at  $r = \varphi_0 = 0$ . For  $\bar{K}_B < 0$ , a finite wavevector instability in bond angle (along with density) occurs at

$$q^* = \pm \frac{|\bar{K}_B|}{\sqrt{3K_C}} \sqrt{1 + \sqrt{1 - 3K_A K_C / \bar{K}_B}}, \quad (6.10)$$

provided  $1/q^*$  is larger than the lattice or disclination cutoff size. The thin dotted lines in Figures 5 and 6 show the possible modulated hexatic phase. Near the critical point, disclination unbinding and melting directly to an isotropic fluid is also possible.

In principle, the solid could melt directly into a modulated hexatic phase via a first order transition. Curves delineating possible hexatic-modulated hexatic and solid-modulated hexatic phase boundaries are shown in Figures 5 and 6.

Provided the gradient coefficient coefficient in (6.7) remains positive the critical point retains non-classical 2D Ising critical behavior. Coupling to bond angle degrees of freedom does not induce the long-ranged elastic interactions that lead to the mean-field critical behavior discussed in Section III.

## ACKNOWLEDGMENTS

We are grateful to D. Frenkel for a preprint of [2] and to B. I. Halperin and C. A. Murray for helpful discussions. This work was supported by the National Science Foundation, primarily through the Harvard Materials Research Science and Engineering Center via DMR-9400396 and in part through grant No. DMR-9417047.

## APPENDIX A: STABILITY ANALYSIS

Bounds on the elastic parameters in Eq. (5.6) follow from a stability analysis in the absence of dislocations. We set  $h = 0$  for simplicity. Two cases must be treated separately. First, we analyze stability with respect to the two components of the displacements  $\vec{u}$ . Then, stability with respect to the three components of zero wavevector strains is checked.

We first write the Fourier transformed Hamiltonian after decomposing the strains into uniform bulk distortions and finite wavevector modes as in Reference [34]. In the decomposition (3.1), the uniform symmetric strains  $u_{ij}^{(0)}$  must be treated separately because these require *three* degrees of freedom, in contrast to the two independent modes when  $\vec{q} \neq 0$ . First consider the finite  $\vec{q}$  contribution to the quadratic part of  $\mathcal{H}$

$$\mathcal{H}_{\vec{q} \neq 0}^{(2)} = \frac{1}{2} \sum_{\vec{q} \neq 0} u_i D_{ij}(\vec{q}) u_j + \frac{1}{2} \sum_{\vec{q} \neq 0} (q^2 + r) |\varphi(\vec{q})|^2 - g \sum_{\vec{q} \neq 0} i q_i u_i \varphi(\vec{q}). \quad (A1)$$

where the phonon dynamical matrix is

$$D_{ij}(\vec{q}) = \mu q^2 \delta_{ij} + (\mu + \lambda) q_i q_j. \quad (A2)$$

The eigenvalues of the quadratic form (A1) are given by

$$\Lambda_{\pm} = \frac{(2\mu + \lambda)q^2 + r + g^2}{2} \pm \frac{1}{2} \sqrt{\frac{\Lambda_0 = \mu q^2}{((2\mu + \lambda)q^2 + r + g^2)^2 - 4(2\mu + \lambda)q^2(r + g^2) + g^2q^2}}. \quad (\text{A3})$$

The onset of instability occurs when an eigenvalue vanishes. Thus, the system is stable against long wavelength ( $q \rightarrow 0$ ) modes when  $\mu > 0$ , and  $r > g^2/(2\mu + \lambda)$ .

For uniform distortions, the quadratic terms in the energy can be written in terms of the three independent components of the strain tensor and  $\varphi$

$$\mathcal{H}_{\vec{q}=0}^{(2)} = \int d^2x \frac{1}{2}(\mu + \lambda)X_+^2 + \frac{\mu}{2}X_-^2 + 2\mu Y^2 + g\varphi X_+ + \int d^2x \frac{r}{2}\varphi^2 \quad (\text{A4})$$

where we have defined

$$\begin{aligned} X_+ &= u_{\ell\ell} \\ X_- &= u_{xx} - u_{yy} \\ Y &= u_{xy} = u_{yx} \end{aligned} \quad (\text{A5})$$

The four eigenvalues in this case are given by

$$\Lambda_{\pm} = \frac{1}{4} \left[ B + r \pm \sqrt{(B - r)^2 + 4g^2} \right], \quad \Lambda_1 = 2\mu, \quad \Lambda_2 = \frac{\mu}{2} \quad (\text{A6})$$

where  $B \equiv \mu + \lambda$ . Stability requires  $\mu > 0$ , and

$$r > g^2/(\mu + \lambda). \quad (\text{A7})$$

Thus, as in a pure elastic theory, the uniform strains impose a more stringent criteria on stability than do the finite wavevector modes. Therefore, as temperature is lowered ( $r = a_2(T - T_c)$ ), the uniform mode  $\varphi_0$  becomes unstable first.

- [1] P. Bolhuis, M. Hagen, and D. Frenkel, Phys. Rev. E **50**(6), 4880, (1994)
- [2] P. Bladon and D. Frenkel, Phys. Rev. Lett., **74**(13), 2519, (1995)
- [3] C. F. Tejero, A. Daanoun, H. N. W. Lekkerkerker and M. Baus, Phys. Rev. E **51**(1), 558, (1995)
- [4] H. Xia, A. L. Ruoff, and Y. K. Vohra, Phys. Rev. B **44**(18), 10374, (1991)
- [5] E. A. Kamenetzky, L. G. Magliocco, H. P. Panzer, Science, **263**, 207, (1994)
- [6] R. J. Hunter, *Foundations of Colloid Science*, vs. I, II, (Oxford, New York, 1992); P. N. Pusey, *Liquids, Freezing and Glass Transition*, J. P. Hansen, D. Levesque, and J. Zinn-Zustin, eds., (North-Holland, Amsterdam, 1991)
- [7] T. Chou and D. R. Nelson, Phys. Rev. E, **48**(6), 4611, (1993)
- [8] D. H. Van Winkle and C. A. Murray, Phys. Rev. **A34**(1), 562, (1986); P. Pansu, P. pieranski, and L. Strzelecki, J. Physique, **44**, 531, (1983); See also *Bond Orientational Order*, edited by K. Strandberg, (Springer, New York, 1991)
- [9] D. Y. C. Chan, J. D. Henry, and L. R. White, J. Coll. Int. Sci., **70**(2), 410, (1981)
- [10] H. N. W. Lekkerkerker and G. J. Vroege, *Phase Transitions in Colloidal Dispersions*, in Fundamental Problems in Statistical Mechanics VIII, Proceedings of the 1993 Altenberg Summer School, (North-Holland, Amsterdam, 1994)
- [11] J. G. Kirkwood, J. Chem. Phys., **7**, 919, (1939)
- [12] V. N. Ryzhov and E. E. Tareyeva, Phys. Rev. B **51**(14), 8789, (1995)
- [13] B. J. Alder and T. E. Wainwright, J. Chem. Phys., **27**, 1208, (1958)
- [14] M. H. J. Hagen and D. Frenkel, J. Chem. Phys., **101**(5), 4093, (1994)
- [15] A. P. Gast, C. K. Hall, and W. B. Russell, J. Coll. Int. Sci., **96**, 251, (1983)
- [16] D. R. Nelson in *Phase Transitions and Critical Phenomena*, v. 7, edited by C. Domb and J. Lebowitz, (Academic Press, London, 1984)
- [17] J. D. Brock, R. J. Birgeneau, J. D. Litster, and A. Aharony, Contemp. Phys., **30**(5), 321, (1989)
- [18] R. Seshadri and R. M. Westervelt, Phys. Rev. B, **46**(9), 5150, (1992); R. Seshadri and R. M. Westervelt, Helv. Phys. Acta (Switzerland), **65**(2-3), 473, (1992)
- [19] D. S. Fisher, B. I. Halperin and R. Morf, Phys. Rev. B **20**,4692, (1979)

- [20] K. Chen, T. Kaplan, and M. Mostoller, Phys. Rev. Lett., **70**(20), 4019, (1995)
- [21] A. Jayaraman, Phys. Rev., **137**, A179, (1965); I. G. Zakrevskii, V. V. Kokorin, and V. A. Chernenko, Soviet Physics, Doklady, **31**(11), 911, (1986); Yu. V. Knyazev, M. M. Kirillova, Yu. I. Kuzmin, and E. Z. Rivman, Soviet J. Low. Temp. Phys., **17**(9), 1143, (1991)
- [22] B. Alder and D. Young, J. Chem. Phys., **70**, 473, (1979)
- [23] J. Y. Wang, D. Vaknin, R. A. Uphaus, K. Kjaer, and M. Losche, Thin Solid Films, **242**(1-2), 40, (1994)
- [24] M. Kosterlitz and D. J. Thouless, J. Phys. C **6**, 1181, (1973)
- [25] N. Goldenfeld, *Lectures on Phase Transitions and the Renormalization Group*, (Addison-Wesley, Reading, MA, 1992); S. K. Ma, *Statistical Mechanics*, (World Scientific, Singapore, 1985)
- [26] L. D. Landau and E. M. Lifshitz, *Theory of Elasticity*, (Pergamon, New York, 1970)
- [27] David R. Nelson, Phys. Rev. **B18**(5), 2318, (1978)
- [28] D. R. Nelson and B. I. Halperin, Phys. Rev. **B19**(5), 2457, (1979)
- [29] A. P. Young, Phys. Rev. B **19**, 1855, (1979)
- [30] D. J. Bergman and B. I. Halperin, Phys. Rev. B **13**, 2145, (1976)
- [31] J. Sak, Phys. Rev. B **10**, 3957, (1974)
- [32] D. R. Nelson, Phys. Rev. B **27**(5), 2902, (1983)
- [33] A. Zippelius, B. I. Halperin, and D. R. Nelson, Phys. Rev. B **22**(5), 2514, (1980)
- [34] A. I. Larkin and S. A. Pikin, Soviet Physics JETP, **29**(5), 891, (1969)
- [35] K. Huang, *Statistical Mechanics*, (Wiley Interscience, New York, 1987)

FIG. 1.  $T - \rho$  phase diagram of a system exhibiting a solid-solid phase coexistence. (CP) is a critical point,  $S_1$  and  $S_2$  are the low and high density solids respectively.

FIG. 2. Interaction potential  $U(\delta)$  between particles and flat confining walls. The distance  $\delta$  along the ordinate measures the distance away from the mid-plane  $\delta = 0.5$  between the walls. When the plates are closely spaced  $U(\delta)$  is given by the dashed curve corresponding to an Ising free energy above critical temperature. Increasing the plate gap lowers the temperature of the Ising-like free energy (solid curve).

FIG. 3. Coexistence of two isostructural solid phases,  $S_1$  and  $S_2$  with lattice constants  $a_+$  and  $a_-$  respectively.

FIG. 4. The solution  $\delta\varphi$  for  $\vec{b} = -b\hat{e}_1$ . Note that  $\varphi$  diverges at the dislocation, and a cutoff must be imposed before  $\delta\varphi$  gets too large; however, unlike the phonon displacement field  $\vec{u}$ ,  $\delta\varphi(\vec{x})$  is single-valued.

FIG. 5. Phase diagram near the critical point of an isostructural solid-solid transition projected on the  $(\bar{r}_0/u, \varphi = \rho - \rho_c)$  plane. For  $\mu = \lambda = 10\pi$ , a lobe of hexatic phase is induced near the critical point. The solid hexatic-solid boundary corresponds to  $g^2/u = 2$ . The hexatic region becomes smaller for smaller  $g^2/u$ . A modulated hexatic phase, evaluated using  $v^2/K_B = 1/45\pi$ , lies within the thin dotted line. The  $S_1 - S_2$  coexistence line is approximated by mean-field theory.

FIG. 6. Phase boundaries projected on the  $\bar{r}_0/u - h/u$  plane for  $\mu = \lambda = 10\pi$  and  $g^2/u = 2.0$ . The smaller lobe corresponding to a modulated hexatic phase is shown by the thin dotted line. A line of discontinuous transitions is represented by the dark line along the  $x$ -axis and a renormalized mean-field critical point is at the origin.

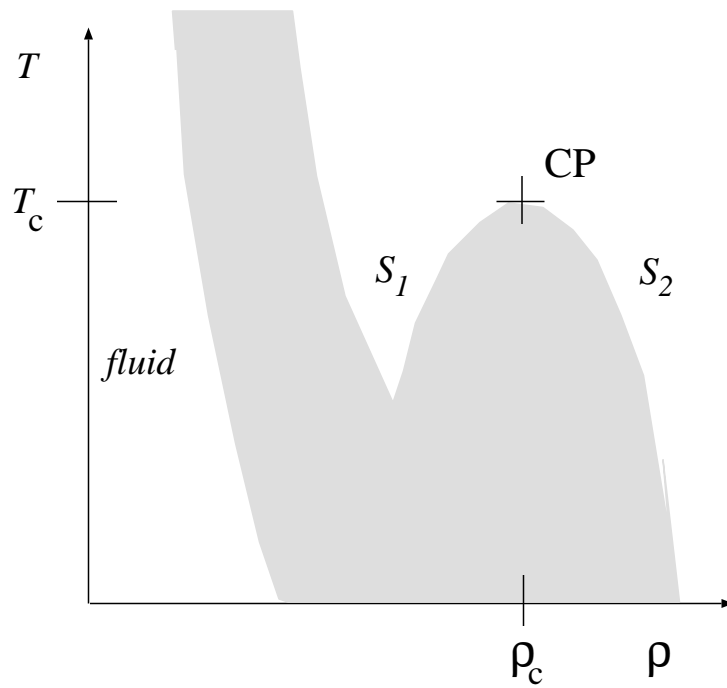


Figure 1

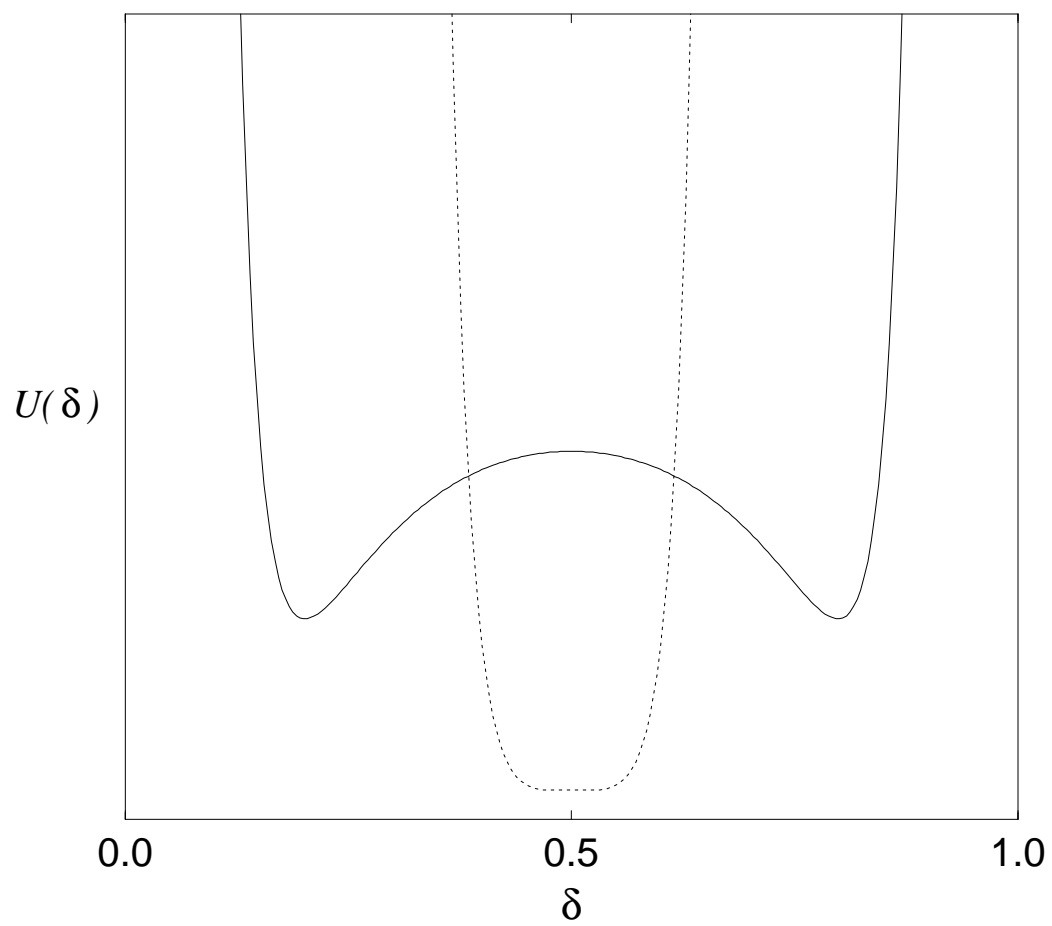


Figure 2

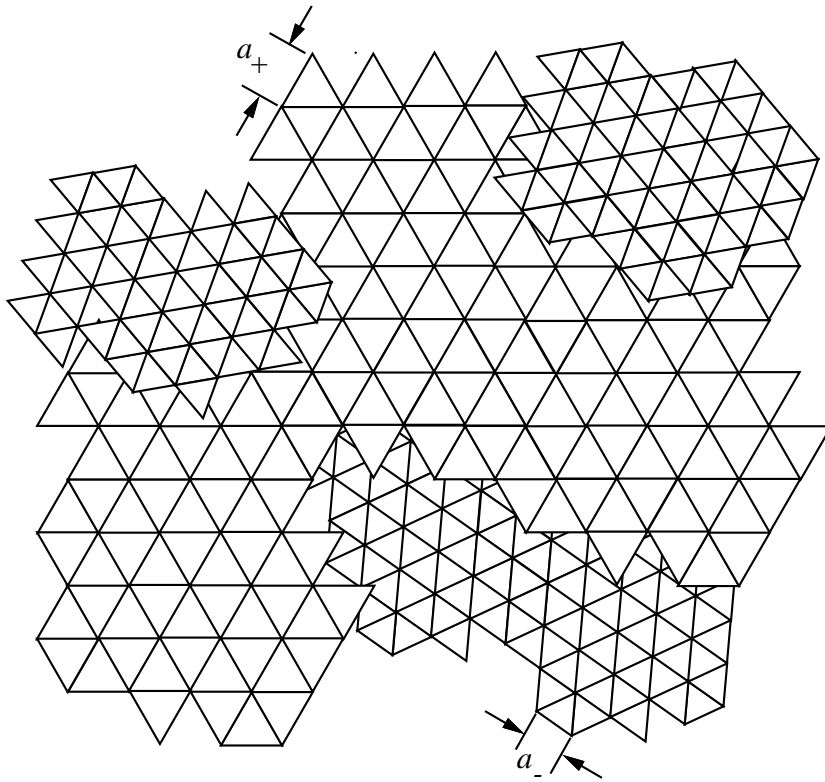


Figure 3

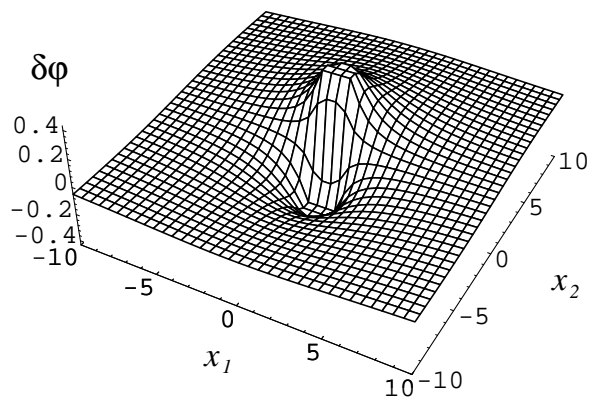


Figure 4



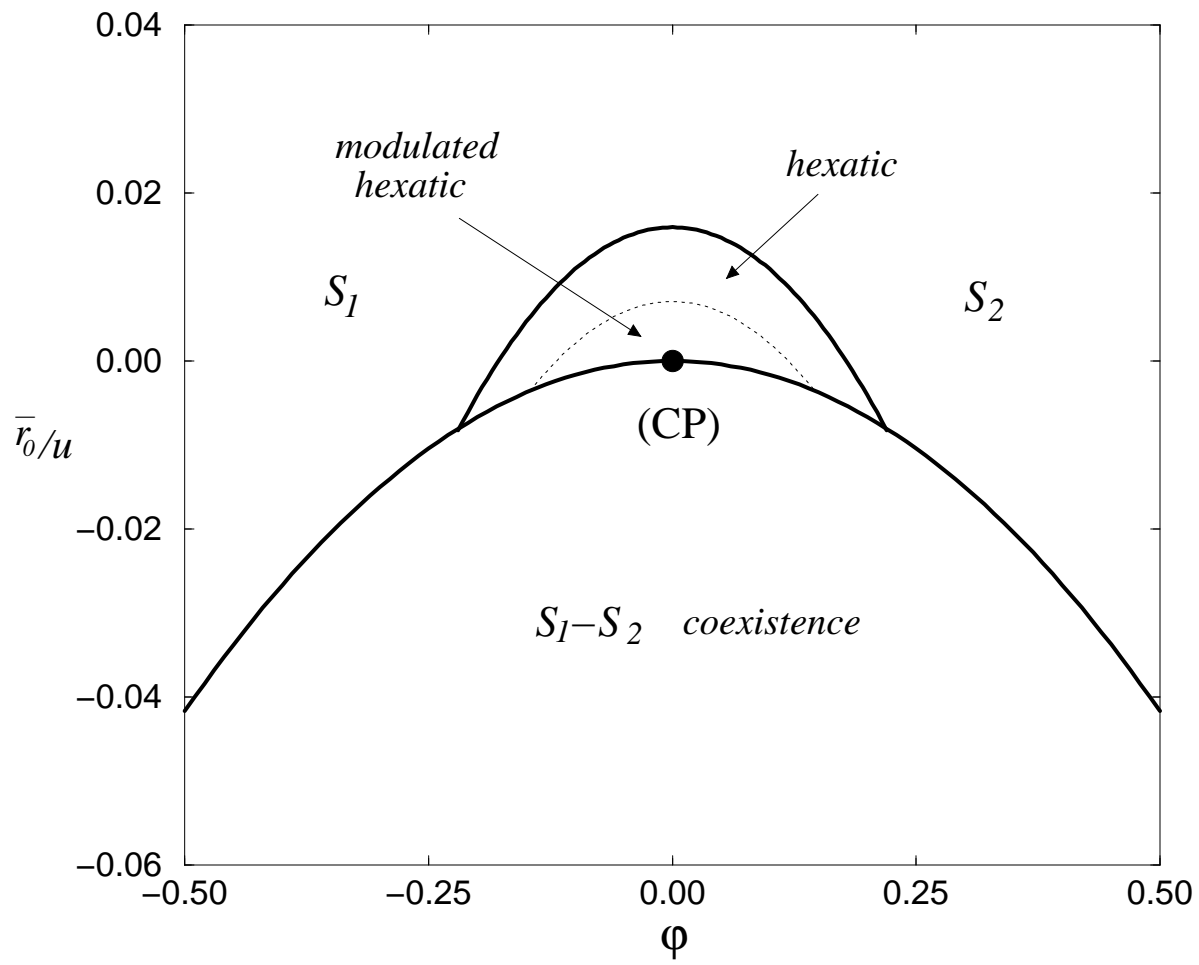


Figure 5

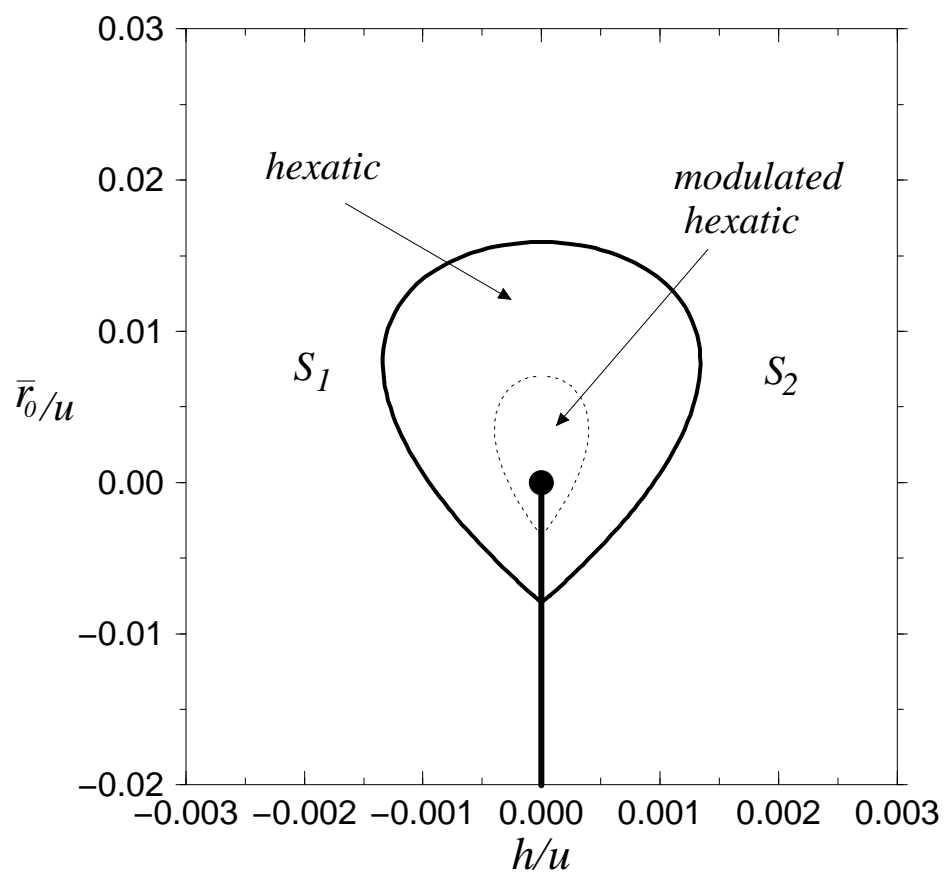


Figure 6